Estimation of water residence time in a permafrost catchment in the Central Tibetan Plateau using long-term water stable isotopic data

Shaoyong Wang[1,2], Xiaobo He[1], Shichang Kang[1,2], Hui Fu[3], Xiaofeng Hong[4]

[1]State Key Laboratory of Cryospheric Science, Northwest Institute of Eco-Environment and Resources, Chinese Academy of
5 Sciences, Lanzhou 730000, China
[2]College of Resources and Environment, University of Chinese Academy of Sciences, Beijing 100049, China
[3]China Institute of Water Resources and Hydropower Research, Beijing 100049, China
[4]Water Resources Department, Yangtze River Scientific Research Institute, Wuhan 430010, China

Correspondence to: Xiaobo He (hxb@lzb.ac.cn)

10 **Abstract.** Global warming has greatly impacted the hydrological processes and ecological environment in permafrost regions. Mean residence time (MRT) is a fundamental catchment descriptor that reveals hydrological information about storage, flow pathways, and water source within a particular catchment. However, water stable isotopes and MRT have scarcely been investigated due to limited data collection in the high-altitude permafrost regions. This study used the long-term stable isotopic observations to identify runoff components and applied the sine-wave exponential model to estimate 15 water MRT in a high-altitude permafrost catchment (5,300 m a.s.l.) in the central Tibetan Plateau (TP). We found that the isotope composition in precipitation, stream, and supra-permafrost water exhibited obvious seasonal variability. Freeze-thaw cycles of permafrost active layer and direct input of precipitation significantly modified the stable isotope compositions in supra-permafrost and stream water. The hydrograph separation revealed that precipitation and supra-permafrost water accounted for 62±13 % and 38±13 % of the total discharge of stream water, respectively. We estimated that MRT for stream 20 and supra-permafrost water was 100 and 255 days, respectively. Such shorter MRT of supra-permafrost and stream water (compared to the non-permafrost catchments) might reflect the unique characteristics of hydrological process in permafrost catchments. Moreover, the MRT of supra-permafrost water was found to be more sensitive to environmental change than that of stream water. Climate and vegetation factors affected the MRT of stream and supra-permafrost water mainly by changing the thickness of permafrost active layer. We conclude that global warming might retard the rate of water cycle in 25 permafrost regions. Overall, our study deepened the understanding of hydrological processes in high-altitude permafrost catchments and provided a decision-making basis for ecological environmental protection and water resources safety in the source of rivers on the TP.

1 Introduction

Permafrost is counted among the regions that are most sensitive to global warming (Wang et al., 2009). The permafrost acts
30 as an aquiclude, which governs the surface runoff and its hydraulic connection with groundwater (Gao et al., 2021). The

spatiotemporal variability of permafrost freeze-thaw cycles alongside the development of an active layer influence the catchment hydrology in a time-dependent manner affecting parameters such as soil water movement direction, storage capacity, and hydraulic conductivity (Gao et al., 2021; Tetzlaff et al., 2018). In the past decades, permafrost has experienced significant, rapid and extensive degradation, which profoundly and extensively affected regional and even continental

35 hydrological regimes, as well as alpine ecology (Cheng et al., 2019; Gao et al., 2021; Jin et al., 2021). This degradation has released valuable meltwater for recharging groundwater (Ma et al., 2019a). The progressive increase of the permafrost active layer thickness has exacerbated the increased water storage capacity of permafrost and exerted a higher contribution of groundwater to river water (Streletskiy et al., 2015). Thus, compared to non-permafrost regions, the presence of an aquiclude and freeze-thaw cycle of the permafrost active layer, contributes to more complex hydrological processes in permafrost

40 regions. However, it remains unclear how permafrost changes would alter water storage and movement in permafrost catchments.

Mean residence time (MRT) is defined as the average time required for input water to travel through water channels and to reach a catchment outlet in either a vertical or a horizontal flow path (McDonnell et al., 2010; Shah et al., 2017). MRT is a fundamental hydraulic descriptor that can be used to reveal information about water storage, flow paths as well as water

45 sources within a particular catchment (Dunn et al., 2007; McGuire and McDonnell, 2006; Shah et al., 2017). Furthermore, catchment water MRT is crucial for examining catchment response to environmental changes (McGuire et al., 2002). Therefore, by quantifying the MRT, the hydrological sensitivity to climatic changes can be identified (Zhou et al., 2021). Moreover, this parameter provides new insights into catchment functions and runoff processes (Farrick and Branfireun, 2015). The influencing factors associated with MRT have been analyzed by previous studies; however, most of them

50 focused on the influencing factors of the catchment area, topographical factors, groundwater contribution, soil properties, and flow path length (Dunn et al., 2007; Ma et al., 2019b; Rodgers et al., 2005c; Soulsby and Tetzlaff, 2008). Therefore, the influence of permafrost changes, climatic factors, and vegetation variations on catchment MRT in a high-altitude permafrost catchment is seldom evaluated. Meanwhile, given the complexities of underlying surface alongside the remoteness and logistical difficulties associated with data collection in high-altitude permafrost catchments, few studies have examined such

55 permafrost catchments to estimate water MRT using isotopic tracers by long time series sampling.

The Tibetan Plateau (TP) is the source region of many large Asian rivers and is often referred as the "Water Tower of Asia". However, the TP is the most vulnerable among the world's water towers under the changing climate in terms of water-supplying role, the downstream dependence of ecosystems, and societal impacts (Immerzeel et al., 2020). The permafrost with the highest elevation and largest area in the mid-latitudes is mainly distributed in the TP, which has experienced

60 significant and extensive degradation (Cheng et al., 2019). The climatic influences of MRT are non-stationary and manifested at an annual scale (Soulsby and Tetzlaff, 2008). Therefore, in this study, we estimated MRT by using long-term

water stable isotopic data (8-year data for stream water and 5-year data for supra-permafrost water) from a high-altitude (5,300 m a.s.l.) permafrost catchment in the central TP. The main objectives of this study were to: (1) characterize isotope composition of the catchment water; (2) elucidate the potential drivers of isotope variations; (3) identify runoff components by using two-component hydrograph separations; (4) estimate an approximation of water MRT of permafrost catchment by using a sine-wave exponential model; and (5) quantify the climate and permafrost changes effects on permafrost hydrological process by using the estimated catchment water MRT. The findings from our study will deepen our understanding of the hydrological process in permafrost regions and will be important for water resources supply and safety in the TP.

2 Materials and methods

2.1 Study area

This study was conducted in the Xiaoliuyu catchment located in the source region of the Yangtze River in the central TP. It has an average altitude of 5,300 m a.s.l. and a drainage area of 2.17 km³, which falls under the transition zone between the monsoon and non-monsoon regions. This study area is unique given the presence of extensive permafrost. In particular, the maximum active layer thickness of permafrost can be > 300 cm, according to the observational data. The area is covered by sedge and wormwood, including species such as *Kobresia capilifolia, Kobresia pygmaea*, and *Kobresia humilis* (Wang et al., 2020a).
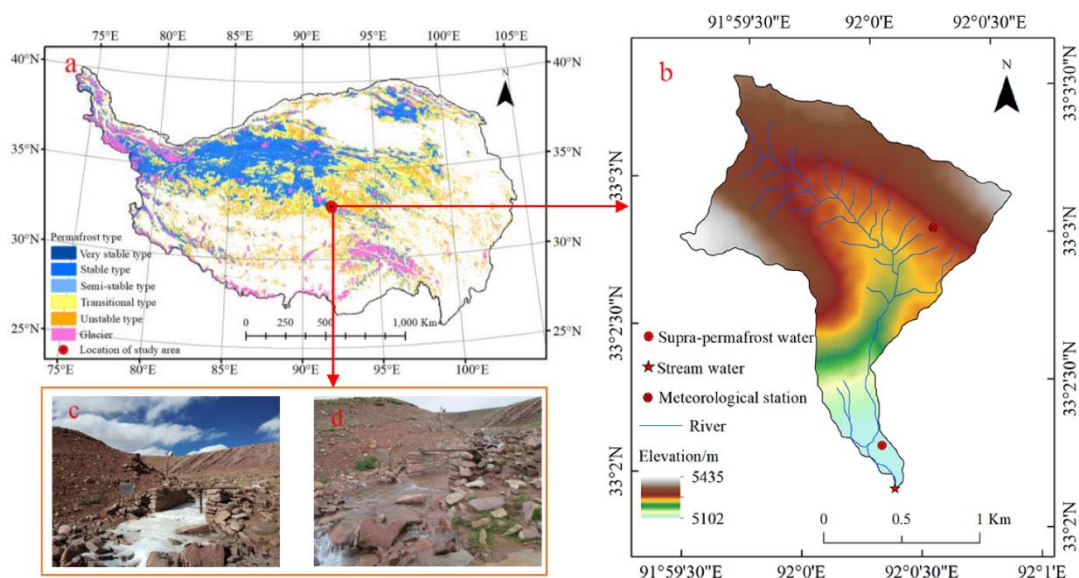
Figure 1. (a) map of permafrost thermal stability on the Tibetan Plateau; (b) map of the study area and the sampling sites; (c-d) images of the frozen river in this catchment during the cold season and the runoff generated during the warm season. Thermal

stability of permafrost distribution data are from National Tibetan Plateau Data Center (TPDC) (http://data.tpdc.ac.cn/) published by Ran et al(2020). Digital Elevation Model (DEM) data available from Geospatial Data Cloud (http://www.gscloud.cn/).
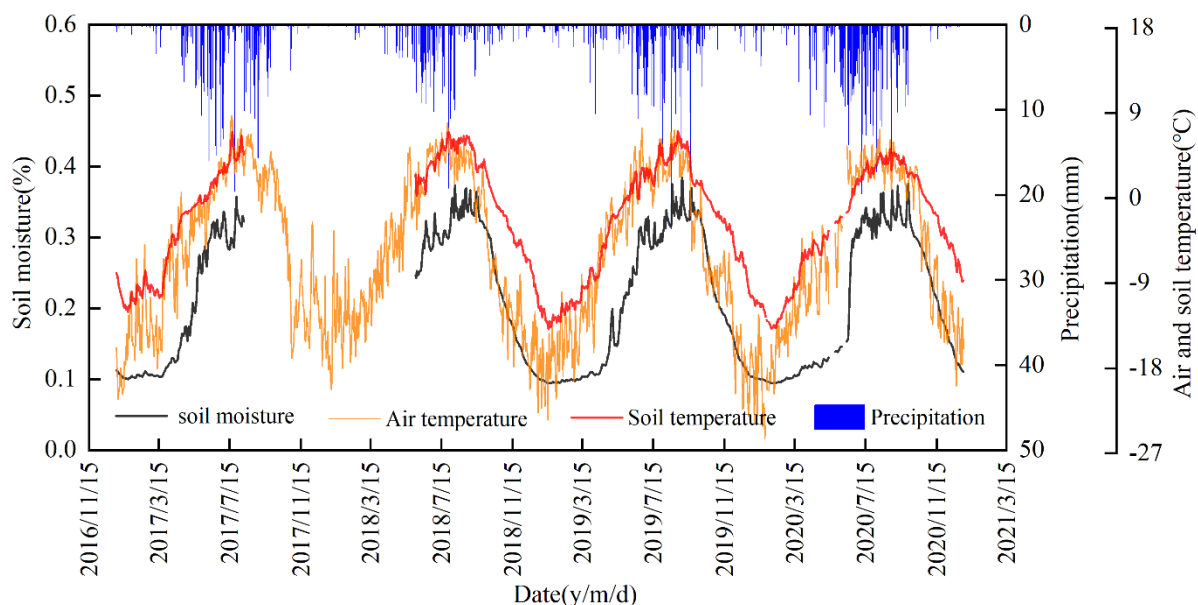
85 **Figure 2. Temporal variation of soil moisture, soil temperature, air temperature, and precipitation from 2017 to 2020.**

2.2 Permafrost and meteorological data

The soil temperature data (active layer bottom temperature) and active layer thickness of permafrost were obtained from the book of *Blue Book on Climate Change in China 2021,* which published long-term data, related to the permafrost in TP (CMA Climate Change Centre, 2021). The normalized differential vegetation index (NDVI) can reflect the growth status

90 and coverage of vegetation. We collected NDVI data from MOD13A2 products provided by the NASA, USA, with temporal and spatial resolutions of 16 days and 1 km × 1 km, respectively (https://ladsweb.modaps.eosdis.nasa.gov/). In our study, the spatial resolution of NDVI data was unified to 25 × 25 m by resampling. The growing-season NDVI was determined using the maximum synthesis method. Meteorological data, including precipitation amount, relative air humidity as well as air temperature are available from the weather stations within the Xiaoliuyu catchment (Fig. 1). The soil temperature, active

95 layer thickness of permafrost, NDVI, and the meteorological data were obtained for 2012–2020, as shown in Table 1.

Table 1. Annual permafrost, normalized differential vegetation index (NDVI), and meteorological data from 2012–2020. The symbol "—" indicates no data were available for that year.

Data type	2012	2013	2014	2015	2016	2017	2018	2019	2020
Active layer thickness (cm)	223	229	228	237	240	240	245	243	237

Soil temperature (℃)	–1.20	–1.19	–1.10	–1.30	–1.00	–0.91	–0.80	–1.31	–1.40
Air temperature (℃)	–5.69	—	–5.97	–4.84	–4.71	–5.00	–5.15	–5.60	–5.50
Precipitation(mm)	527	547	674	307	541	486	319	455	626
Relative humidity (%)	53.78	—	54.8	49.03	50.37	53.55	53.32	57.38	56.29
NDVI	0.2312	0.1336	0.1362	0.1842	0.1880	0.1771	0.1400	0.1807	0.1769

2.3 Field sampling and isotope analysis

100   Note that the high sampling frequency can more efficiently identify substantial modification of the catchment hydrology and can provide more information of hydrological processes (Stockinger et al., 2016). In this study, the continuous sampling and high sampling frequency of stream water, supra-permafrost water, and precipitation were conducted from June to October. The sampling sites are shown in Figure 1. and detailed information of sampling sites is summarised in Table 2.

In total, the 416 precipitation samples were collected during the observation period in bulk collectors at the Tanggula

105   Cryosphere and Environment Observation Station (TaCOS), Chinese Academy of Sciences at the altitude of 5,050 m a.s.l. The precipitation samples were immediately collected after every precipitation event to reduce the impact of evaporation. The groundwater in the permafrost region can be classified into three categories: supra-permafrost water, intra-permafrost water as well as sub-permafrost water (Cheng and Jin, 2013; Gao et al., 2021). Supra-permafrost water is the most widely distributed groundwater type in the permafrost regions of TP, which is mainly stored in the permafrost active layer (Li et al.,

110   2020). We collected 755 stream water samples and 296 supra-permafrost water samples at approximately 1-day intervals in the Xiaoliuyu catchment from June to October for each year (Fig. 1b). As the stream water and the permafrost layer are frozen due to low temperature in the cold season, the stream and supra-permafrost water is simply generated during the warm season (Fig. 1c and d). The supra-permafrost water samples were taken from a well, that was drilled at a depth of 1.5 m. Given the logistical constraints in this study area, only a single stream and supra-permafrost water sampling site were

115   collected.

All samples were collected in individual 50-ml PE bottles that were rinsed three times with the water from the source itself before sampling. The bottles were then sealed and stored in a refrigerator at a temperature of –10℃ to minimize the possibility of contamination from the external environment and isotopic fractionation, induced by liquid water evaporation. Hydrogen (δD) and oxygen (δ^{18}O) stable isotopes composition of all water samples were measured by Liquid-Water Isotope

120   Analyzer (DLT 100, Los Gatos, USA) at the State Key Laboratory of Cryospheric Sciences, Chinese Academy of Sciences. The water samples were analyzed six times. The first two results were discarded to eliminate "memory effects", and the average of the last four results was used as the isotope estimate of the water samples. The results were reported in per mil (‰) units relative to the Vienna Standard Mean Ocean Water (V-SMOW). The precision of measurement for δ^{18}O and δD was ± 0.2 ‰ and ± 0.6 ‰, respectively.

125

Table 2. Information of samples and sampling sites.

Sample type	Years	Altitude (m a.s.l.)	No. of samples
Precipitation	2012, 2014–2020	5129	416
Stream water	2012, 2014–2020	5139	756
Supra-permafrost water	2012, 2017–2020	5146	296

2.4 Isotope hydrograph separation method

The isotopic hydrograph separation (IHS) method is based on a mass balance approach. It can be used to estimate the contributions of diverse sources to terminal water using isotope (δ^{18}O or δD) as a tracer (Uhlenbrook and Hoeg, 2003; Yuzhong et al., 2018). The method can be formalized by using Eqs. (1) and (2), shown below:

$$Q_s = Q_p + Q_e, \tag{1}$$
$$Q_s C_s = Q_p C_p + Q_e C_e, \tag{2}$$

where Q_s, Q_p and Q_e represent stream water, pre-event (supra-permafrost water) and event water (precipitation) volumes, respectively; C_s, C_p and C_e are the corresponding values of δ^{18}O or δD. The contributions of pre-event water and event water to stream water can be calculated by combining Eqs. (1) and (2) to obtain Eqs. (3) and (4):

$$f_p = \frac{C_e\text{-}C_t}{C_e\text{-}C_p} \times 100\%, \tag{3}$$

$$f_e = \frac{C_t\text{-}C_p}{C_e\text{-}C_p} \times 100\%, \tag{4}$$

where f_p and f_e represent relative contribution ratio of pre-event water and event water to stream water, respectively. The uncertainty of the calculated fractions of event and pre-event water was evaluated using the Gaussian error propagation technique (Uhlenbrook and Hoeg, 2003).

2.5 Estimation of mean residence times

Earlier studies have demonstrated that the sine-wave exponential model can be used to estimate MRT using the seasonal variations of isotope composition in precipitation and stream water (Ma et al., 2019b; McGuire et al., 2002; McGuire and McDonnell, 2006; Soulsby and Tetzlaff, 2008; Zhou et al., 2021). Mathematically, the movement of conservative tracer through a catchment can be expressed by the convolution integral (McGuire and McDonnell, 2006; Simin et al., 2013), which states that the tracer concentration of output water $\delta_{\text{out}}(t)$ at any time and input tracer $\delta_{\text{in}}(t\text{-}\tau)$ that enter uniformly into the catchment in the past $t\text{-}\tau$, which becomes lagged by its transit time distribution g(τ). The common transit time distribution model g(τ) used in hydrologic systems include: exponential, exponential-piston flow, and dispersion models (Simin et al., 2013). In our study, the exponential model was used to estimate water MRT:

$$\delta_{out}(t) = \int_0^{\infty} g(\tau)\,\delta_{in}(t-\tau)\,\mathrm{d}\tau, \tag{5}$$

$$g(\tau) = \tau_m^{-1}\exp(\frac{\tau}{\tau_m}), \tag{6}$$

where τ is the transit time, t is the time of tracer exit from the catchment and t-τ represents the time of tracer enter into the catchment, τ_m is mean residence time (MRT).

In our study, the seasonal variations of $\delta^{18}O$ were modelled using sine-wave function to fit the seasonal $\delta^{18}O$ variations in precipitation, supra-permafrost water, and stream water, defined by Eq. (7):

$$\delta(t) = X + A\left[\cos\left(ct - \theta\right)\right], \tag{7}$$

where $\delta(t)$ is the modelled $\delta^{18}O$ (‰), X is the mean measured $\delta^{18}O$ (‰), A is the amplitude of the measured $\delta^{18}O$, c is the radial frequency constant given as $c=2\pi/153$ days$=0.04105$ rad d^{-1} in our study (the total number of days from June to October considered in this study amounted to 153) and θ is the phase lag of modelled $\delta^{18}O$ in radians. The overall performance of the sine-wave model was evaluated by using the goodness of fit (R^2) and root mean square error (RMSE).

Analytical solution of the MRT (τ_m) for the exponential model can be derived by combining Eq. (5) with Eq. (7) (McGuire and McDonnell, 2006):

$$MRT = c^{-1}\sqrt{\left[\left(\frac{A_{z1}}{A_{z2}}\right)^{-2} - 1\right]}, \tag{8}$$

where A_{Z1} is the amplitude of precipitation $\delta^{18}O$, A_{Z2} is the amplitude of modelled $\delta^{18}O$ in supra-permafrost or stream water in our study, and c is the radial frequency, defined in Eq. (7). The uncertainty of the MRT estimates were quantified by determining the 95% confidence of the fitted sine-wave's amplitude. Specifically, applying the 95% confidence of the fitted sine-wave's amplitude to Eq. (8) producing MRT error (the upper and lower 95% confidence boundaries of the estimated MRT) (Morales and Oswald, 2020).

3 Results and discussion

3.1 Stable isotope composition and δD-$\delta^{18}O$ relationships of precipitation, stream, and supra-permafrost water

The hydrological examination can benefit from the following phenomenon. Meteoric water is the main driver of hydrological processes at the catchment scale, while the hydrogen and oxygen isotope composition in different waters are correlated (Chiogna et al., 2014). For a detailed examination of the differences of isotopic composition in the different waters and their mutual transformation, the relationships between $\delta^{18}O$ and δD for precipitation, stream water, and supra-permafrost water were quantified (Fig. 3).

During the sampling periods, the isotopic composition in precipitation (−30.9 to 2.9 ‰ for $\delta^{18}O$; −244.2 to 34 ‰ for δD) strongly varied, compared with that in stream water (−19.6 to −4.0 ‰ for $\delta^{18}O$; −146.3 to −39.8 ‰ for δD) and in supra-

permafrost water (−17.5 to 4.6 ‰ for δ^{18}O; −127.6 to 50.9 ‰ for δD) (Table 3). This finding indicates that precipitation was an important recharge source for supra-permafrost and stream water in the analyzed permafrost catchment. We identified the

180 substantial difference among the water line in different water: the stream water (SWL: δD=6.66δ^{18}O-7.61 ‰), supra-permafrost water (PWL: δD=6.10δ^{18}O-15.89 ‰), and local meteoric water line (LMWL: δD=8.01δ^{18}O+13.48 ‰). The lower slopes of SWL (6.66) and PWL (6.1) strikingly indicate the non-equilibrium fractionation caused by evaporation, reducing the slope of δD-δ^{18}O correlation line (Xia et al., 2021). Alternatively, we surmise that there could be precipitation mixed with water from previous events stored in the permafrost active layer. In contrast, supra-permafrost water exhibited the lower

185 slope, which was most likely caused by thawing and freezing of the active soil layer (Wang et al., 2009). This can be explained by the longer residence time of water in the permafrost active layer, resulting in lower slope of water lines. These findings are similar to previous results obtained for the Zuomaokong watershed in the hinterland of the TP (Song et al., 2017). Hence, the lower slope of the water line of supra-permafrost water may indicate relatively longer catchment water MRT.

190 **Table 3. Mean, range, and standard deviation of δ^{18}O (‰) and δD (‰) for precipitation, stream water, and supra-permafrost water.**

Sample type	Mean		Minimum		Maximum		Standard deviation	
	δ^{18}O	δD	δ^{18}O	δD	δ^{18}O	δD	δ^{18}O	δD
Precipitation	−13.2	−92.6	−30.9	−244.2	2.9	34.0	7.1	58.0
Supra-permafrost water	−14.0	−101.5	−17.5	−127.6	−4.6	50.9	1.7	10.8
Stream water	−13.5	−97.4	−19.6	−146.3	−4.0	−39.8	2.4	16.3
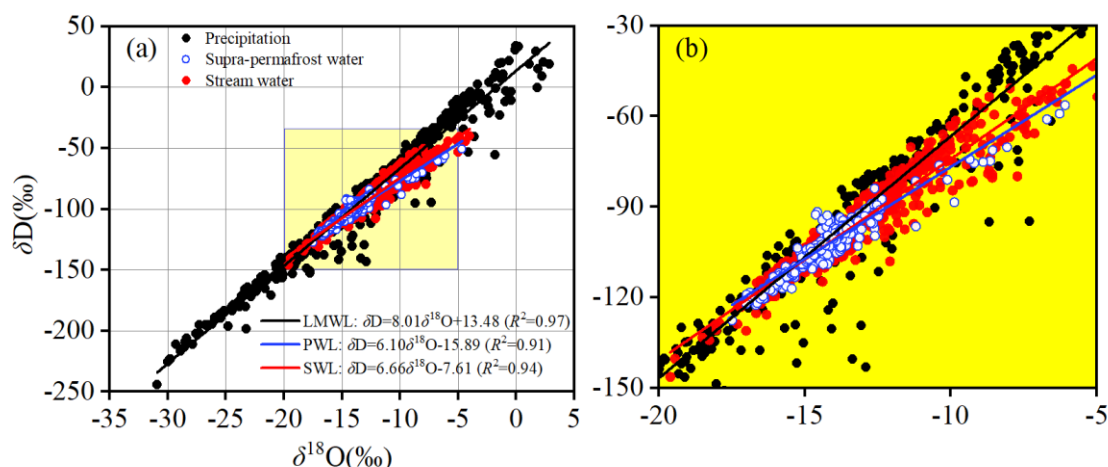
Figure 3. Relationships between δ^{18}O and δD of precipitation, stream water, and supra-permafrost water. (a) all isotope data; (b) the data, constrained by yellow square.

3.2 Temporal variations of stable isotopes in stream and supra-permafrost water and their potential drivers

The variations of $\delta^{18}O$ and δD compositions in different water samples exhibited similar tendencies, as seen in Figure 3. Due to this, $\delta^{18}O$ was selected as the representative isotope in the following analysis. The temporal variations of $\delta^{18}O$ in stream and supra-permafrost water are shown in Figure 4. The analysis revealed that substantial seasonal variability of stable isotope signature was identified in different waters. The precipitation isotopes deplete heavy isotopes during the period of the Indian summer monsoon (from late May to early September) and enrich heavy isotopes at the beginning and end of the summer monsoon period (late May and mid-October). This pattern is similar to those of the monsoon region of the southern TP, due to the shifting moisture source between the Bay of Bengal and the southern Indian Ocean (Yao et al., 2013). The stream water samples also exhibited a depletion in the isotopic signature, which is virtually consistent with the precipitation results from the overall variation trend (Fig. 4). The isotope compositions in supra-permafrost water for the certain year (such as 2018 and 2019) also reflected the isotope signals of precipitation, but exhibited the least variability for overall supra-permafrost water (lowest standard deviation shown in Table 3), compared to precipitation and stream water. This finding suggests that mixing processes within the active layer attenuate variations of $\delta^{18}O$ signal from precipitation.
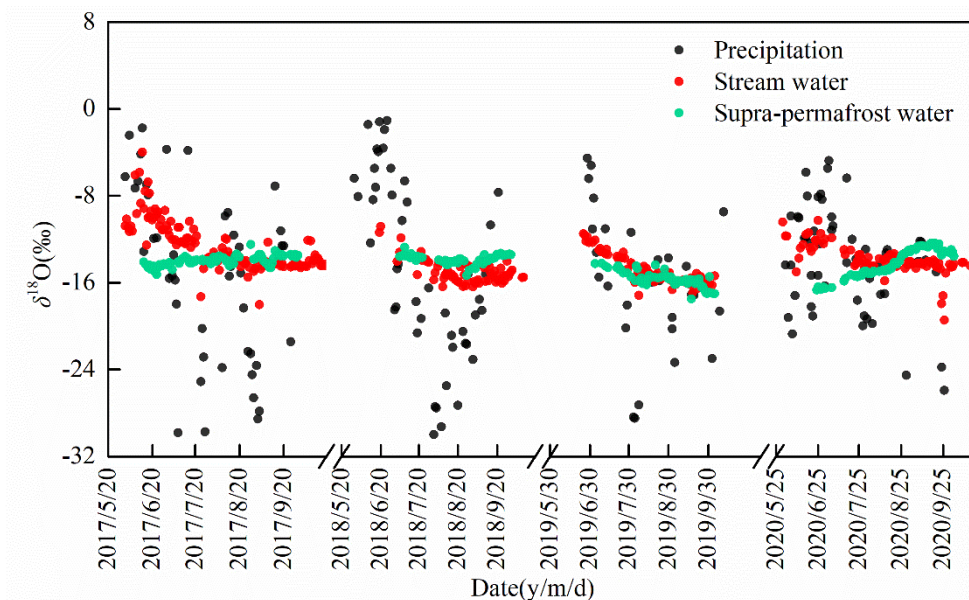
Figure 4. Comparison of variations of precipitation $\delta^{18}O$ (‰), stream and supra-permafrost water δ18O (‰) during the warm seasons from 2017 to 2020.

The seasonal dynamics of the soil temperature and moisture of the active layer are the most important drivers of hydrological processes in the permafrost regions (Wang et al., 2009; Wang et al., 2015). In our study area, the stable isotope compositions in supra-permafrost and stream water may have been significantly altered by the freeze-thaw cycle of permafrost active layer. Hence, we conducted the correlation analysis between the isotope compositions in supra-permafrost and stream water, as well as soil temperature and soil moisture (Fig. 5).

The correlation analysis revealed that the isotopic compositions in stream water are negatively correlated with soil temperature (Pearson's correlation coefficient (r)=−0.316, $P<0.01$) and soil moisture (r=−0.560, $P<0.01$). They are also strongly positively correlated with the isotopic compositions in precipitation (r=0.644, $P<0.01$). These findings indicate that the stream water was controlled by precipitation and freeze-thaw cycle of the permafrost active layer. Notably, our

220 correlation results are in line with the previous studies in the Zuomaokong watershed of central TP (Song et al., 2017). Although this may be related to the fact that thawing of permafrost releases frozen soil water that depleted in isotopes. But previous study found that melting ground ice in permafrost was not a source of the observed runoff variations, but rather the thickening of the active layer (Landerer et al., 2010).

The isotopic compositions in supra-permafrost water were found to be significantly associated with soil temperature
225 (r=0.201, $P<0.01$). Moreover, we identified a variable relationship between the supra-permafrost water isotopes and soil temperature (first increasing and then decreasing) (Fig. 6). A similar relationship was observed for soil moisture (but not significant). When soil temperature was <4℃, the active layer was relatively thinner, and less water was stored in the permafrost active layer, which is more susceptible to evaporation, causing isotope enrichment. With the further increase of soil temperature (>4℃), the active layer becomes thicker and the soil moisture also increases, yielding the supra-permafrost
230 water recharged by greater amounts of precipitation that depleted in isotopes (precipitation depleted heavy isotopes in August). The positive correlation between supra-permafrost water with precipitation isotope (r=0.510, $P<0.01$), and the negative correlation between precipitation isotope with soil temperature (r=−0.447, $P<0.01$) and with soil moisture (r=−0.564, $P<0.01$) also confirms this finding. Our results present isotopic evidence that the thawing of the permafrost active layer is essential for the hydrologic processes in permafrost catchments.

235 In contrast, the isotope compositions in stream water were much more responsive to precipitation than to supra-permafrost water. As the active layer of permafrost can effectively store precipitation and the groundwater storage is a long-term accumulation of local precipitation. Thus, the isotope compositions in groundwater generally express integrative characteristics of seasonal precipitation inputs, which are less sensitive to the recharge of precipitation. However, the stream water is mostly affected by seasonal precipitation, thereby, somewhat following the variability of precipitation characteristics.
240 This indicates that precipitation was essential for stream water, whereas the freezing and thawing process of the active layer was pivotal in controlling supra-permafrost water, which reflects the influence of permafrost as a specific surface aquifer on the hydrological process.
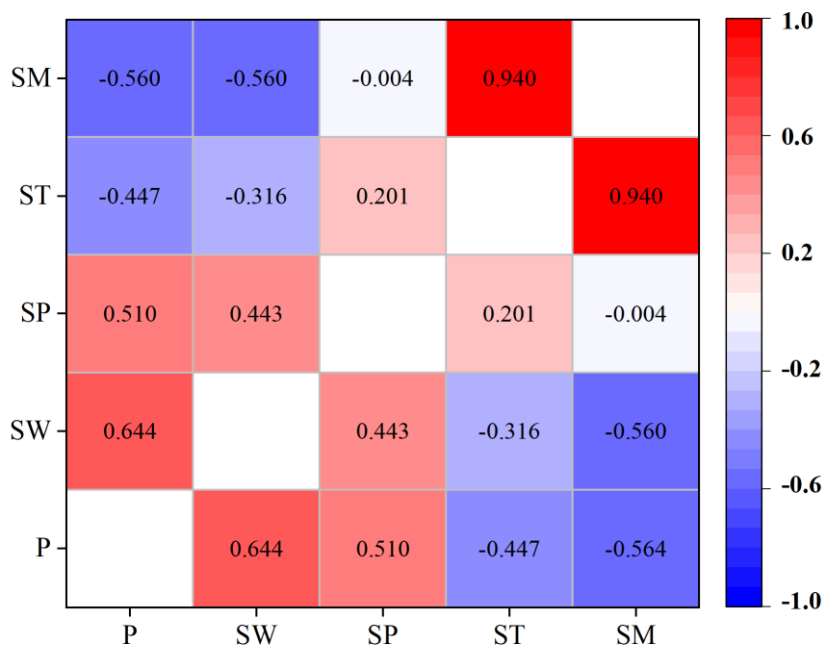
Figure 5. Correlation analysis between stable isotopes and influencing factors. Coloured rectangle shows the significance of the correlation (P<0.01). The larger the value and the darker the colour the more significant of the correlation between variables. Abbreviations: P = Precipitation δ^{18}O (‰); SW = Stream water δ^{18}O (‰); SP = Supra-permafrost water δ^{18}O (‰); ST = Soil temperature (℃); SM = Soil moisture (%).
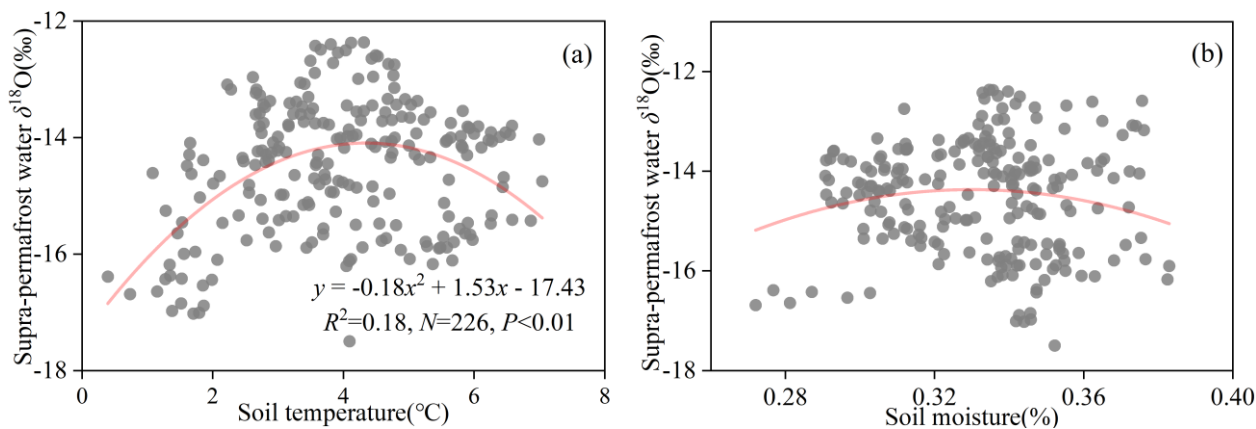
Figure 6. Correlation between δ^{18}O in supra-permafrost water with: (a) soil temperature (b) soil moisture.

3.3 Two-component hydrograph separations of stream water

The differences of the isotopic composition and water lines between the different waters allow distinguishing the sources of stream water. In this study, compared with supra-permafrost water (−14.0 ‰), the average precipitation δ^{18}O value (−13.2 ‰)

is closer to that of stream water (−13.5 ‰) points on the dominant recharge of precipitation to stream water (Table 3). For quantitative evaluation of the results above, the source proportion of stream water was quantitatively determined by using the isotopic data and the IHS model (Eqs. 1–4). The results indicate that precipitation and supra-permafrost water contributed 62±13 % and 38±13 % of the total discharge of stream water, respectively. This finding further suggests that precipitation was the dominant component of the stream water during the warm season. Similar previous studies have reported that precipitation and thawing permafrost water contributes 55.2 % and 44.8 % to thermokarst lakes in the Beiluhe basin of the interior of the TP (4,600 m a.s.l.) (Yang et al., 2016). However, a recent study has demonstrated that a greater contribution of supra-permafrost water (49 %), compared with precipitation (34 %) in the whole source region of the Yangtze River (Li et al., 2020). We further found that the contribution rate of supra-permafrost water to stream water in our catchment was relatively less, compared with the downstream area and the whole source region of the Yangtze River. This identified pattern is potentially related to higher amount of precipitation (491.9 mm) and the steeper slope in our catchment. Notably, this is more conducive to generating a large amount of runoff into the river channel. Alternately, the higher supra-permafrost water contribution to river water could include that of the cold season (Li et al., 2020), but there was no supra-permafrost water generated during the cold season in our study area in the whole source region of the Yangtze River.

3.4 Estimation of mean residence time using seasonal variability of water isotopes

The modelled amplitudes can reflect the observed patterns of variability of water isotope compositions due to great mixing; meanwhile, seasonal variations in the output waters are far more significant with larger amplitude, thereby, indicating greater responsiveness to recent precipitation inputs (Rodgers et al., 2005a). In this study, the analysis in the first three subsections above manifested that precipitation has an important input to stream and supra-permafrost water, which provides a prerequisite for the evaluation of residence time by using sine-wave exponential model. Thus, we fit seasonal sine-wave curves to the annual $\delta^{18}O$ variations in precipitation, stream, and supra-permafrost water. The sine-wave regression parameters for $\delta^{18}O$ in precipitation, supra-permafrost water, and stream water are shown in Figure 7–9. We found that the modelled $\delta^{18}O$ fit well to the observed isotope values, with RMSE of 4.35–6.58 ‰ for precipitation, 0.37–1.95 ‰ for supra-permafrost water, and 0.72–1.99 ‰ for stream water. Meanwhile, the results of periodic regression analysis of isotope compositions in different waters were all statistically robust ($P < 0.01$). The $\delta^{18}O$ seasonal variations of supra-permafrost and stream water exhibited weak amplitudes, compared with the precipitation, which is a consequence of the mixing processes and longer residence time. The mean amplitude of stream water (1.54 ‰) in our study reasonably agrees with the previous results in the Zuomaokong watershed of hinterland of the TP (1.76 ‰), which applied the same method to calculate the mean amplitude of stream water $\delta^{18}O$ in five permafrost catchments (Song et al., 2017).
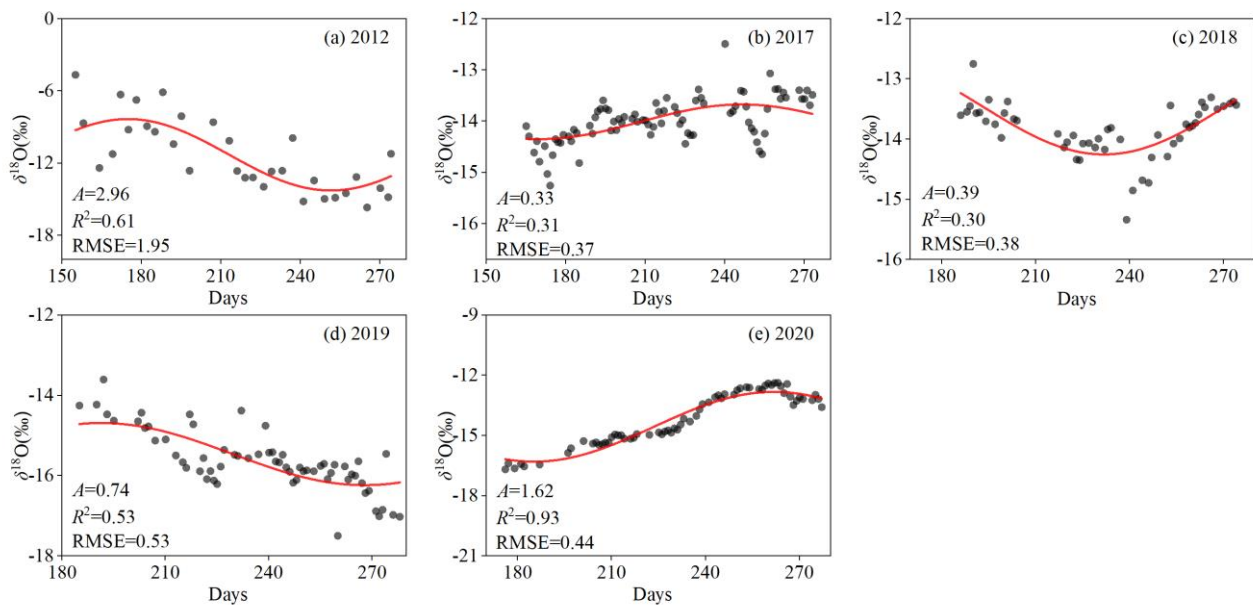
Figure 7. Fitted sine–wave regression models to δ^{18}O in supra-permafrost water in Xiaoliuyu catchment during 2012, 2017-2020. A is the amplitude and RMSE is root mean square error for the modelled isotopic signature.
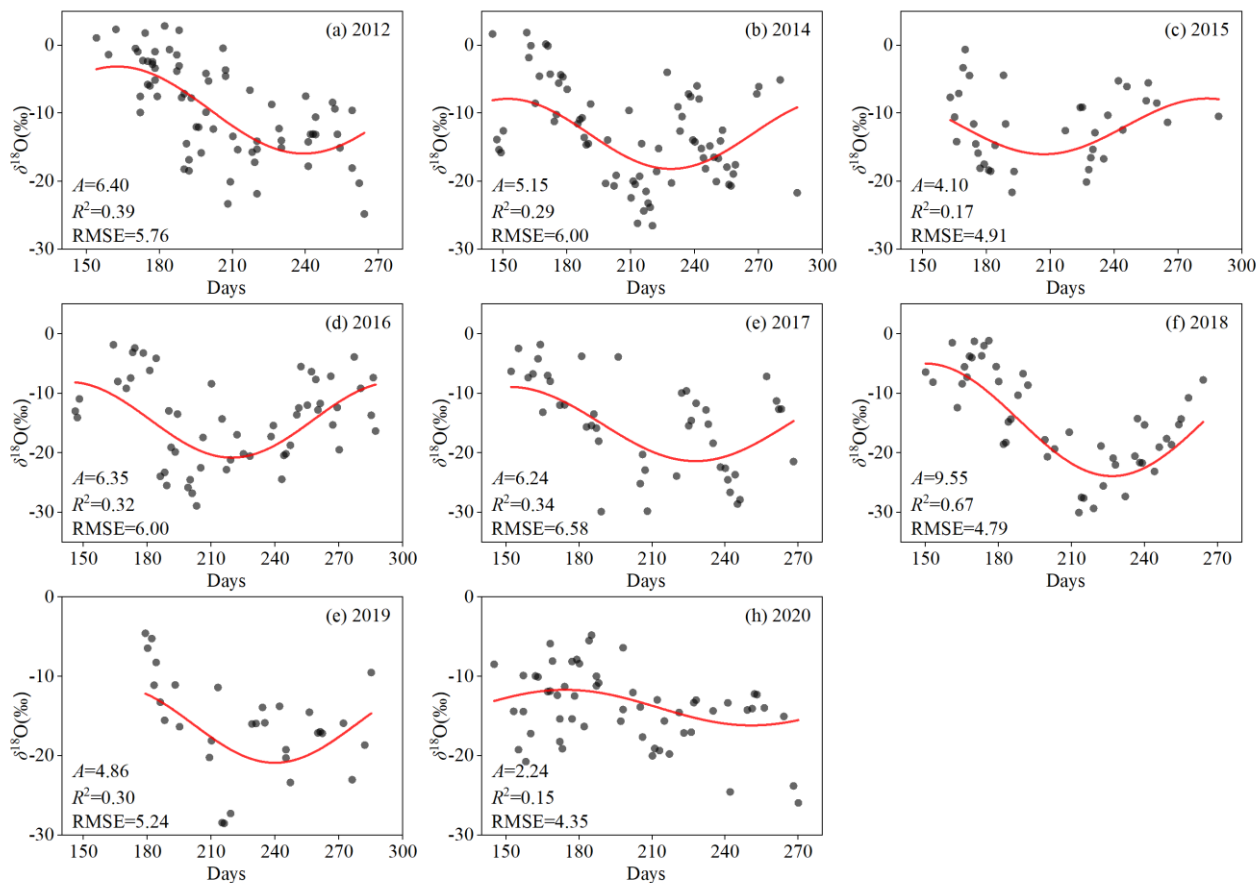
Figure 8. Fitted sine-wave regression models to δ^{18}O in precipitation in Xiaoliuyu catchment during 2012, 2014–2020. A is the amplitude and RMSE is root mean square error for the modelled isotopic signature.

290
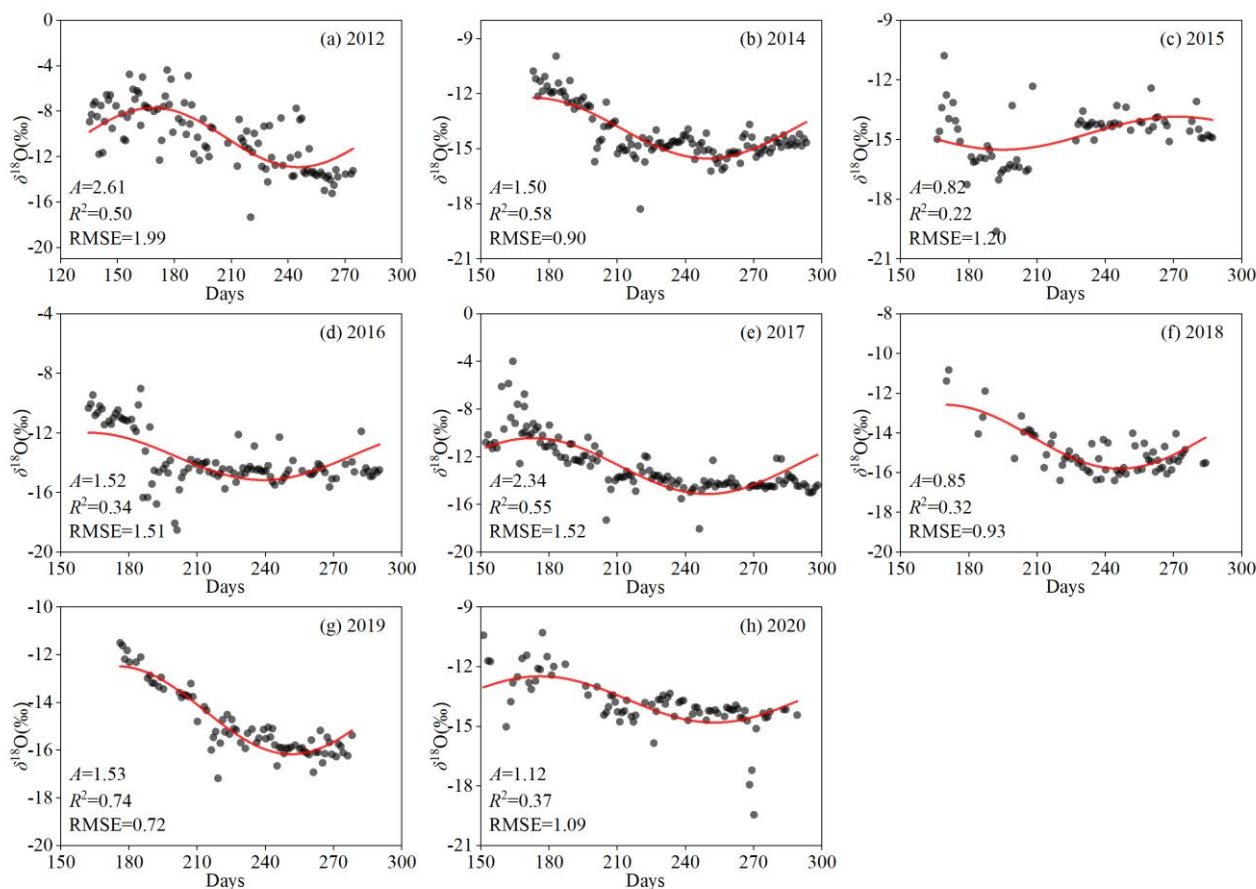
Figure 9. Fitted sine-wave regression models to $\delta^{18}O$ in stream water in Xiaoliuyu catchment during 2012, 2014–2020. A is the amplitude and RMSE is root mean square error for the modelled isotopic signature.

Then, the sine-wave regression parameters were translated into the estimates of water MRT by using Eq. (6). The estimated

295 results of MRT are shown in Figure 10. The calculated MRT for the stream water ranged from 42 to 270 days, with a mean value of 100 days and a standard deviation of 68 days. Meanwhile, for supra-permafrost water, the MRT varied from 23 to 596 days, with a mean value of 255 days and a standard deviation of 229 days. The estimated MRT revealed a large annual variability, regardless of stream water or supra-permafrost water. It should be noted that the estimated MRT of supra-permafrost water was distinctly longer than that of stream water. The longer MRT reflects more complex soil water retention

300 and recharge processes (Ma et al., 2019b). In turn, a short MRT of the stream water indicates a relatively rapid response of surface water to precipitation. The estimated MRT of stream and supra-permafrost water in our catchment were shorter, compared to those estimated in most previous studies from non-permafrost or high-latitude permafrost catchments (Table 4). This may be related to whether there is groundwater recharge or not. Permafrost acts as an aquiclude, while being usually characterized by rapid hydrograph responses (Tetzlaff et al., 2018). Moreover, it cuts off the interaction and mixing between

305   deep groundwater and surface water and supra-permafrost water. For instance, (Rodgers et al., 2005b; Soulsby et al., 2006) have reported that catchment water MRT was correlated with the percentage groundwater contributions to stream water in non-permafrost catchment. Furthermore, previous studies have revealed longer MRT for deep groundwater (Table 4). For instance, the MRT of the mixture of supra-permafrost and intra-permafrost water ranges from ~1 to 55 years in the permafrost regions of the Arctic region (Hiyama et al., 2013). In particular, deep groundwater MRT in the mountainous

310   Brugga basin ranged from 6 to 9 years (Uhlenbrook et al., 2002). Thus, the mixing or interaction between stream water and groundwater increases the stream water MRT in the non-permafrost catchments. However, this interaction is suspended by the permafrost layer in our catchment, causing the shorter MRT. This implies that the hydrological processes in high-altitude permafrost region are unique, compared with non-permafrost or high-latitude permafrost regions.

Table 4. Statistics of MRT-related research results. The symbol "—" indicates no data were available in the references.

Site	Altitude (m a.s.l.)	Land type	Water type	MRT	References
Our study site	5100–5435	Permafrost	Stream water	100 days	This study
Siksik Creek	50–100	Permafrost	Stream water	548 days	(Tetzlaff et al., 2018)
Mandava	383	Non-permafrost	Stream water	444 days	(Sanda et al., 2017)
Allt Mharcaidh	699	Non-permafrost	Stream water	263–445 days	(Rodgers et al., 2005a)
Upper Váh	1500	Non-permafrost	Stream water	390–570 days	(M. et al., 2011)
Dee	1000	Non-permafrost	Stream water	600 days	(Soulsby et al., 2010)
Minjiang	300–7100	Non-permafrost	Stream water	293–870 days	(Xia et al., 2021)
Our study site	5100–5435	Permafrost	Groundwater	255 days	This study
Lena River	130–160	Permafrost	Groundwater	1–55 years	(Hiyama et al., 2013)
Himalaya	1600–5200	Non-permafrost	Groundwater	4.5 months	(Shah et al., 2017)
Vermigliana	1221	Non-permafrost	Groundwater	1.3 years	(Chiogna et al., 2014)
Allt a' Mharcaidh	300–1111	Non-permafrost	Groundwater	>5 years	(Soulsby et al., 2000)
Brugga	434–493	Non-permafrost	Groundwater	6–9 years	(Uhlenbrook et al., 2002)
Karst	—	Non-permafrost	Groundwater	161–1407 days	(Wang et al., 2020b)

315
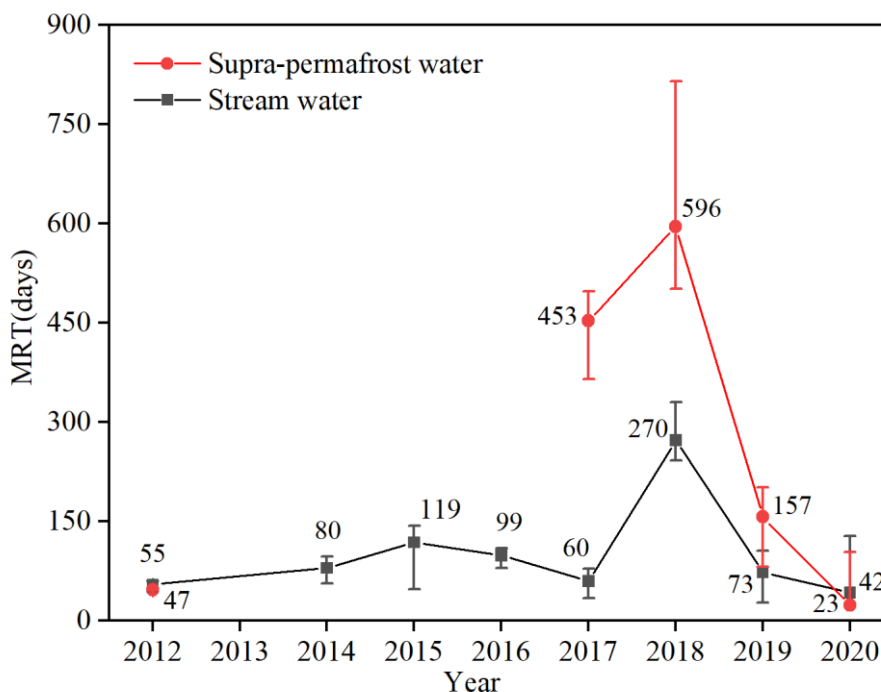
Figure 10. Inter-annual variation of stream water MRT during 2012, 2014–2020, and supra-permafrost water MRT during 2012, 2017–2020.

3.5 Factors determining the MRT of stream and supra-permafrost water

320 Theoretically, multiple factors affect the water storage in the active layer, including precipitation and soil temperature in permafrost regions (Wright et al., 2008). The climate differences and variability may have substantially affected the MRT estimates (Tetzlaff et al., 2007). Table 5 shows the quantified correlations between estimated MRT and soil parameters (active layer thickness and soil temperature), climate factors (air temperature, precipitation, and relative humidity) and vegetation index as well (NDVI).

325 As the buffer layer between the permafrost and atmosphere, the active layer is vulnerable to climate change (Xu and Wu, 2021). The increase of air temperature can alter the temperature of shallow permafrost due to strong land surface-atmosphere interactions. This, in turn, induces an increase of the active layer thickness of permafrost, allowing soil water to be moved and stored in the deeper soil layer. The correlation analysis showed that the MRT of supra-permafrost water exhibits a strong positive correlation with air temperature ($R^2 = 0.90$) and soil temperature ($R^2 = 0.77$) (Table 5). These strong correlations

330 indicate that soil and air temperature are potentially efficient predictors of supra-permafrost water MRT. In contrast, the relatively weaker positive correlations were identified between stream water MRT and air temperature ($R^2 = 0.16$) and soil temperature ($R^2 = 0.38$). Moreover, we observed that MRT of supra-permafrost and stream water were negatively weakly correlated with the active layer thickness ($R^2 = 0.35$ and 0.23, respectively). The deeper active layer somewhat triggers longer

catchment water MRT, because the increase of the thickness of active layer increases the soil and deeper flow paths, thereby

335 slowing the catchment water response to the precipitation. In addition, the deeper active layer allows more water to be stored, precluding the accumulation of soil moisture deficits. These results also support the findings from previous studies in terms of a relationship between permafrost changes and residence time. In particular, (Wright et al., 2009) have stated that MRT of permafrost catchments is highly dependent on the annual development of the active layer. Moreover, (Lyon et al., 2010) have reported that the potential thaw of permafrost layers due to climate change could increase MRT at the catchment scale

340 by 20–45 %. A similar study in the non-frozen regions reported that MRT of forestland and shrubland water both increased with soil depth (Ma et al., 2019b).

Precipitation is an important part of the water cycle and is the main input for catchment water sources. However, precipitation in the permafrost region of TP significantly increased in recent decades (Zhao et al., 2019). Does increased precipitation affect runoff processes in permafrost watersheds? In our study, the longest estimated MRTs (270 days for

345 stream water and 596 days for supra-permafrost water) were observed in 2018 with the relatively lower precipitation amount (319 mm). We analyzed the correlation between MRT and precipitation and relative humidity and found that supra-permafrost and stream water MRT are both negatively correlated with precipitation (R^2= 0.69 and 0.49, respectively) (Table 5). Moreover, supra-permafrost water MRT also has a relatively weak negative correlation with relative humidity (R^2= 0.36) (Table 5). This indicates the increased precipitation and wetter climatic conditions may accelerate the water cycle process in

350 permafrost regions. The larger precipitation corresponds to lower temperature, yielding a thinner active layer, which, in turn making the active layer water to be saturated sooner. This phenomenon subsequently triggers more water to rapidly flow into the river channel in the form of surface runoff, thereby, reducing the MRT of catchment water in the end. However, previous study suggested that much wetter climate than average probably causes higher MRT in the low-altitude temperate regions (Soulsby et al., 2006). Our study does not resonate with these results, possibly because the aquiclude effect of permafrost

355 reduces surface infiltration and enhances surface runoff generation (Gao et al., 2021).

Soil layer is the main source of nutrients and water required for vegetation growth (Xu et al., 2019). Water shortage in soil layer may occur when water MRT is too short, but longer MRT can hamper the water infiltration consequently to root anoxia, thus, affecting the plant growth (Ma et al., 2019b). Interestingly, we found that the stream and supra-permafrost water MRT are both negatively correlated with NDVI (R^2= 0.29 and 0.53, respectively) (Table 5). Alternatively, an increase in

360 vegetation coverage (high NDVI values) might lead to a longer MRT in our catchment. Previous studies have noted the vegetation cover was one of the most important factors, that governs the hydrological processes and thermal cycles in permafrost catchment (Wang et al., 2012b) . The decline of vegetation coverage induced increases of soil temperature and moisture, at which they accelerate the active soil thawing (Wang et al., 2012a). Therefore, the effect of vegetation on MRT is actually driven by the variations of thickness of the permafrost active layer. However, it remains unclear whether a

365   positive feedback mechanism exists between vegetation and permafrost active layer changes or not. Moreover, the optimum

residence time for vegetation growth should be elucidated in future studies as well.

In this study, comparisons of the controlling factors of MRT between stream and supra-permafrost water indicated that

supra-permafrost water is more sensitive to environmental change, compared with stream water. Previous studies suggested

that supra-permafrost water in the seasonally thawed layer is sensitive to climate (Cheng and Jin, 2013), and is, therefore,

370   significantly impacted by precipitation, temperature, and vegetation. From the influencing mechanism perspective, climate

and vegetation factors affected the MRT of stream and supra-permafrost water by modifying the active layer thickness of

permafrost. It can be deduced that the estimated MRT of supra-permafrost water is valuable for evaluating the extent of

permafrost degradation. Most importantly, it can be used to infer the effects of long-term climate, permafrost changes, and

vegetation on the hydrologic regime in permafrost regions.

375   **Table 5. Correlations between active layer thickness, soil temperature, air temperature, precipitation, relative humidity, NDVI, and MRT. *x* indicates the factor as the independent variable.**

Factor	Stream water	Supra-permafrost water
Active layer thickness(cm)	$y = 4.63x - 995.14$ $R^2 = 0.23$	$y = 3\text{E}{-}8\text{e}^{0.0943x}$ $R^2 = 0.35$
Soil temperature (°C)	$y = 211.96x + 339.02$ $R^2 = 0.38$	$y = 929.35x + 1300.1$ $R^2 = 0.90$
Air temperature (°C)	$y = 1231.1\text{e}^{0.5049x}$ $R^2 = 0.16$	$y = 752.19x + 4307.9$ $R^2 = 0.77$
Precipitation (mm)	$y = 378.76\text{e}^{-0.003x}$ $R^2 = 0.49$	$y = -1.90x + 1169.7$ $R^2 = 0.69$
Relative humidity (%)	$y = -7.62x + 508.03$ $R^2 = 0.08$	$y = -83.38x + 4829.4$ $R^2 = 0.36$
NDVI	$y = -1288.6x + 327.59$ $R^2 = 0.27$	$y = -5723.6x + 1292.2$ $R^2 = 0.53$

4 Conclusions

In this study, long-term observational stable isotopic data were used to estimate water MRT in a high-altitude permafrost

catchment of the TP. We found that the isotope composition in precipitation, stream and supra-permafrost water exhibited

380   obvious seasonal variability. The freeze-thaw cycles of permafrost active layer and direct input of precipitation significantly

modified the stable isotope compositions in the supra-permafrost and stream water. The two-component IHS model indicated

that the precipitation was the main contribution to the total discharge of stream water. We estimated that the MRT ranged

from 42 to 270 days (mean 100 days) and 23 to 596 days (mean 255 days) for stream water and supra-permafrost water,

respectively. These results can be compared with the previous findings, reported in non-permafrost catchments. Namely,

385   evaluation of seasonal variations of stable isotope composition can be efficiently applied to estimate water MRT in high-

altitude permafrost catchment. Furthermore, the analysis of influencing factors revealed that the MRT of supra-permafrost

water was more sensitive to environmental change than stream water. From the perspective of influencing mechanisms,

climate and vegetation factors affected the water MRT in permafrost catchment which were mainly driven by changing the

thickness of the permafrost active layer. It should be emphasized that the estimated MRT of supra-permafrost water is
390   valuable for evaluating the extent of permafrost degradation. Under the influence of global warming, the permafrost degenerates and active layer deepens may slow down the rate of water cycle in permafrost regions.

Although our study has confirmed that isotope techniques can be utilized to estimate the MRT of water in high-altitude permafrost catchments, there were some limitations. As the hydrological investigation at high-altitude region was very challenging, we only conducted long-term isotope monitoring on one sub-catchment, which may result in sampling biases.

395   Thus, it is necessary to utilize more measurements in different sub-catchments to augment the representativeness of the research. Future work is required to evaluate the impact of topography and soil property on water MRT in permafrost catchments. To conclude, our study provided unique insights and will encourage further research in permafrost regions. Our findings will deepen the understanding of hydrological processes in high-altitude permafrost catchments and provide a decision-making basis for ecological environmental protection and water resource safety and exploitation in the source of

400   rivers on the TP.

Data availability. We have uploaded the long-term isotope data and estimated MRT results in figshare with the URL of https://figshare.com/articles/dataset/IsoMRTTP/19172765.

Author contribution. XH and SK provided initial ideas of this work. SW and XH performed the water isotope data collection and processing and result analysis. XH provided the meteorological data of the study area. HF and XFH helped in analyzing

405   the results and revised the manuscript. All authors contributed to the writing.

Competing interests. The authors declare that they have no conflict of interest.

Acknowledgements. This work was supported by the Joint Research Project of Three-River Headwaters National Park, Chinese Academy of Sciences and the People's Government of Qinghai Province (LHZX-2020-11), the Second Tibetan Plateau Scientific Exploration (Grant 2019QZKK0605), IWHR Research & Development Support Program

410   (HY110145B0012021) and the project of State Key Laboratory of Cryospheric Science (SKLCS-ZZ-2022).

References

Cheng, G., Zhao L., Li, R., Wu X., Sheng, Y., Hu, G., Zou, D., Jin, H., Li, X., and Wu Q.: Characteristic, changes and impacts of permafrost on Qinghai-Tibet Plateau, Chinese Science Bulletin, 64, 2783–2795, 2019.

Cheng, G. D and Jin, H. J.: Groundwater in the permafrost regions on the Qinghai-Tibet Plateau and it changes,

415   Hydrogeology & Engineering Geology, 40, 1–11, https://doi.org/10.16030/j.cnki.issn.1000-3665.2013.01.017, 2013.

Chiogna, G., Santoni, E., Camin, F., Tonon, A., Majone, B., Trenti, A., and Bellin, A.: Stable isotope characterization of the Vermigliana catchment, Journal of Hydrology, 509, 295-305, https://doi.org/10.1016/j.jhydrol.2013.11.052, 2014.

Climate Change Centre.: Blue Book on Climate Change in China, Beijing: Science Press, 2021.

Dunn, S. M., McDonnell, J. J., and Vaché, K. B.: Factors influencing the residence time of catchment waters: A virtual experiment approach, Water Resources Research, 43, 1639-1650. https://doi.org/10.1029/2006WR005393, 2007.

Farrick, K. K and Branfireun, B. A.: Flowpaths, source water contributions and water residence times in a Mexican tropical dry forest catchment, Journal of Hydrology, 529, 854–865, https://doi.org/10.1016/j.jhydrol.2015.08.059, 2015.

Gao, H., Wang J., Yang Y., Pan X., and Duan Z.: Permafrost Hydrology of the Qinghai-Tibet Plateau: A Review of Processes and Modeling, Frontiers in Earth Science, 8, 1–13, https://doi.org/10.3389/feart.2020.576838, 2021.

Hiyama, T., Hiyama, T., Asai, K., Kolesnikov, A., Gagarin, L., and Shepelev, V.: Estimation of the residence time of permafrost groundwater in the middle of the Lena River basin, eastern Siberia. Environmental Research Letters, 8, https://doi.org/10.1088/1748-9326/8/3/035040, 2013.

Immerzeel, W., Immerzeel, W. W., Lutz, A. F., Andrade, M., Bahl, A., and Baillie, J.: Importance and vulnerability of the world's water towers, Nature, 577, 364–369, https://doi.org/10.1038/s41586-019-1822-y, 2020.

Jin, X. Y., Jin, H. J., Iwahana, G., Smarchenko, S., Luo, D. L., Li, X.Y., and Liang, S. H.: Impacts of climate-induced permafrost degradation on vegetation: A review, Advances in Climate Change Research, 12, 29–47, https://doi.org/10.1016/j.accre.2020.07.002, 2021.

Wang, L., He, X., Fsteiner, J., Zhang, D. W., Wu, J., Wang, S. Y., and Ding,Y. J.: Models and measurements of seven years of evapotranspiration on a high elevation site on the Central Tibetan Plateau, Journal of Mountain Science, 17, 3039–3053, https://doi.org/10.1007/s11629-020-6051-1, 2020.

Landerer, F. W., Dickey, J. O., and Güntner, A.: Terrestrial water budget of the Eurasian pan-Arctic from GRACE satellite measurements during 2003–2009, Journal of Geophysical Research: Atmospheres, 115, https://doi.org/10.1029/2010JD014584, 2010.

Li, X., He X., Kang, S., Mika, Sillanp., Ding, Y., Han T., Wu, Q., and Yu, Z.: Diurnal dynamics of minor and trace elements in stream water draining Dongkemadi Glacier on the Tibetan Plateau and its environmental implications, Journal of Hydrology, 541, 1104-1118, https://doi.org/10.1016/j.jhydrol.2016.08.021, 2016.

Li, Z., Li, Z., Qi, F., Zhang, B., and Gao, W.: Runoff dominated by supra-permafrost water in the source region of the Yangtze river using environmental isotopes, Journal of Hydrology, 582, https://doi.org/10.1016/j.jhydrol.2019.124506, 2020.

Lyon, S. W., Steve W. Lyon., Hjalmar Laudon., Jan Seibert., Magnus Mrth., Doerthe Tetzlaff., and Kevin H. B.: Controls on snowmelt water mean transit times in northern boreal catchments, Hydrological Processes, 24, https://doi.org/10.1002/hyp.7577, 2010.

Dosa, M., Holko, L., and Kostka, Z.: Estimation of the mean transit times using isotopes and hydrograph recessions, Die Bodenkultur, 62, 47–52, 2011.

450   Ma, J., Song, W., Wu, Jinkui., Liu, Z., and Wei, Z: Identifying the mean residence time of soil water for different vegetation
types in a water source area of the Yuanyang Terrace, southwestern China, Isotopes in Environmental and Health
Studies, 55, 1–18, https://doi.org/10.1080/10256016.2019.1601090, 2019.

Ma, Q., Jin, H. J., Bense, V. F., Luo, D. L., and Lan, Y. C.: Impacts of degrading permafrost on streamflow in the source
area of Yellow River on the Qinghai-Tibet Plateau, China, Advances in Climate Change Research, 10, 225–239,
455   https://doi.org/10.1016/j.accre.2020.02.001, 2019.

McDonnell, J. J.; McGuire, K.; Aggarwal, P.; Beven, K. J.; Biondi, D.; Destouni, G.; Dunn, S.; James, A.; Kirchner, J.; and
Kraft, P.: How old is streamwater? Open questions in catchment transit time conceptualization, modelling and analysis,
Hydrological Processes, 24, 1745–1754, https://doi.org/10.1002/hyp.7796, 2010.

McGuire, K. J.; DeWalle, D. R.; and Gburek, W. J.: Evaluation of mean residence time in subsurface waters using oxygen-
460   18 fluctuations during drought conditions in the mid-Appalachians, Journal of Hydrology, 261, 132–149, 2002.

McGuire, K. J and McDonnell, J. J.: A review and evaluation of catchment transit time modeling. Journal of Hydrology, 330,
543–563, https://doi.org/10.1016/j.jhydrol.2006.04.020, 2006.

Morales, K and Oswald, C.: Water age in stormwater management ponds and stormwater management pond treated
catchments. Hydrological Processes, 34, 1854–1867, https://doi/10.1002/hyp.13697, 2020.

465   Ran, Y., X Li., G Cheng., Z Nan., and X Wu.: Mapping the permafrost stability on the Tibetan Plateau for 2005-2015,
Science China Earth Sciences, 63, 62–79, https://doi.org/10.1007/s11430-020-9685-3, 2020.

Rodgers, P., Soulsby, C., and Waldron, S.: Stable isotope tracers as diagnostic tools in upscaling flow path understanding
and residence time estimates in a mountainous mesoscale catchment. Hydrological Processes, 19, 2291–2307,
https://doi.org/10.1002/hyp.5677, 2005a.

470   Rodgers, P., Soulsby, C., Waldron, S., and Tetzlaff, D.: Using stable isotope tracers to assess hydrological flow paths,
residence times and landscape influences in a nested mesoscale catchment. Hydrology and Earth System Sciences, 9,
139–155, https://doi.org/10.5194/hess-9-139-2005, 2005b.

Martin, Š., Pavlína, S., Tomáš, V., Christina, S., Matthias, K., Jakub, J., Alena, K., and František, P.: Pre-event water
contributions and streamwater residence times in different land use settings of the transboundary mesoscale Lužická
475   Nisa catchment, Journal of Hydrology and Hydromechanics, 65, 154-164, https://doi.org/10.1515/johh-2017-0003,
2017.

Shah, R., Jeelani, G., and Noble, J.: Estimating mean residence time of karst groundwater in mountainous catchments of
Western   Himalaya,   India.   Hydrological   Sciences   Journal,   62,   1230–1242,
https://doi.org/10.1080/02626667.2017.1313420, 2017.

480   Qu, S., Tao, W., Bao, W., Peng, S., Peng, J., Zhou, M., and Yu Z.: Evaluating Infiltration Mechanisms Using Breakthrough
Curve and Mean Residence Time, Water Resources Management, 27, 4579–4590, https://doi.org/10.1007/s11269-013-
0427-8, 2013.

Song, C., Wang, G., Liu, G., Mao, T., Sun, X., and Chen, X.: Stable isotope variations of precipitation and streamflow reveal the young water fraction of a permafrost watershed, Hydrological Processes, 31, 935–947, https://doi.org/10.1002/hyp.11077, 2017.

Soulsby, C., R. Malcolm., R. Helliwell., R. C. Ferrier., and A. Jenkins.: Isotope hydrology of the Allt a' Mharcaidh catchment, Cairngorms, Scotland: implications for hydrological pathways and residence times, Hydrological Processes, 14, 747-762, https://doi.org/10.1002/(SICI)1099-1085(200003)14:4<747::AID-HYP970>3.0.CO;2-0, 2000.

Soulsby, C and Tetzlaff, D.: Towards simple approaches for mean residence time estimation in ungauged basins using tracers and soil distributions, Journal of Hydrology, 363, 60–74, https://doi.org/10.1016/j.jhydrol.2008.10.001, 2008.

Soulsby, C., Tetzlaff, D., and Hrachowitz, M.: Spatial distribution of transit times in montane catchments: conceptualization tools for management, Hydrological Processes, 24, 3283–3288, https://doi.org/10.1002/hyp.7864, 2010.

Soulsby, C., Tetzlaff, D., Rodgers, P., Dunn, S., and Waldron, S.: Runoff processes, streamwater residence times and controlling landscape characteristics in a mesoscale catchment: an initial assessment, Journal of Hydrology, 325, 197–221, 2006.

Stockinger, M. P., Bogena, H. R., Lücke, A., Diekkrüger, B., Cornelissen, T., and Vereecken, H.: Tracer sampling frequency influences estimates of young water fraction and streamwater transit time distribution, Journal of Hydrology, 541, 952–964, https://doi.org/10.1016/j.jhydrol.2016.08.007, 2016.

Streletskiy, D., Tananaev, N., Opel, T., Shiklomanov N., Nyland, K., Streletskaya, I., Tokarev, I., and Shiklomanov, A.: Permafrost hydrology in changing climatic conditions: Seasonal variability of stable isotope composition in rivers in discontinuous permafrost, Environmental Research Letters, 10, 095003, https://doi.org/10.1088/1748-9326/10/9/095003, 2015.

Tetzlaff, D., Malcolm, I. A., and Soulsby, C.: Influence of forestry, environmental change and climatic variability on the hydrology, hydrochemistry and residence times of upland catchments, Journal of Hydrology, 346, 93-111, https://doi.org/10.1016/j.jhydrol.2007.08.016, 2007.

Tetzlaff, D., Piovano, T., Ala-Aho, P., Smith, A., Carey, S. K.., Marsh, P., Wookey, P. A., Street, L. E., and Soulsby, C.: Using stable isotopes to estimate travel times in a data-sparse Arctic catchment: Challenges and possible solutions. Hydrological Processes, 32, 1936–1952. https://doi.org/10.1002/hyp.13146, 2018.

Uhlenbrook, S., Frey, M., Leibundgut, C., and Maloszewski, P.: Hydrograph separations in a mesoscale mountainous basin at event and seasonal timescales, Water Resources Research, 38, https://doi.org/10.1029/2001WR000938, 2002.

Uhlenbrook, S and Hoeg, S.: Quantifying uncertainties in tracer-based hydrograph separations: a case study for two-, three- and five-component hydrograph separations in a mountainous catchment, Hydrological Processes, 17, 431–453, https://doi.org/10.1002/hyp.1134, 2003.

Wang F., Chen H., Lian J., Fu Z., and Nie Y.: Seasonal recharge of spring and stream waters in a karst catchment revealed by isotopic and hydrochemical analyses, Journal of Hydrology, 591, https://doi.org/10.1016/j.jhydrol.2020.125595, 2020.

Wang, G., Hu, H., and Li, T.: The influence of freeze-thaw cycles of active soil layer on surface runoff in a permafrost watershed, Journal of Hydrology, 375, 438–449, https://doi.org/10.1016/j.jhydrol.2009.06.046, 2009.

520   Wang, G., L, G., and Chunjie.: Effects of changes in alpine grassland vegetation cover on hillslope hydrological processes in a permafrost watershed, Journal of Hydrology, 444–445, 22–33. https://doi.org/10.1016/j.jhydrol.2012.03.033, 2012a.

Wang G., Liu G., Li C., and Yan Y.: The variability of soil thermal and hydrological dynamics with vegetation cover in a permafrost region, Agricultural and Forest Meteorology, 162-163, 44–57, https://doi.org/10.1016/j.agrformet.2012.04.006, 2012b.

Wang, G., Mao, T., Chang, J., and Liu, G.: Soil temperature-threshold based runoff generation processes in a permafrost
525   catchment, The Cryosphere Discussions, 9, 5957-5978, https://doi.org/10.5194/tcd-9-5957-2015, 2015.

Wright, N., Hayashi, M., and Quinton, W. L.: Spatial and temporal variations in active layer thawing and their implication on runoff generation in peat-covered permafrost terrain, Water Resources Research, 45. https://doi.org/10.1029/2008WR006880, 2009.

Wright, N., Quinton, W. L., and Hayashi, M.: Hillslope runoff from an ice-cored peat plateau in a discontinuous permafrost
530   basin, Northwest Territories, Canada, Hydrological Processes, 22, 2816–2828, https://doi.org/10.1002/hyp.7005, 2008.

Xia, C., Liu, G., Zhou, J., Meng, Y., and Mei, J.: Revealing the impact of water conservancy projects and urbanization on hydrological cycle based on the distribution of hydrogen and oxygen isotopes in water, Environmental Science and Pollution Research, 28, 1–18, https://doi.org/10.1007/s11356-020-11647-6, 2021.

Xu, H., Qu, Q., Peng, L., Guo, Z., and Wulan, E.: Stocks and stoichiometry of soil organic carbon, total nitrogen, and total
535   phosphorus after vegetation restoration in the Loess Hilly Region, China, Forests, 10, 27, https://doi.org/10.3390/f10010027, 2019.

Xu, X and Wu, Q.: Active layer thickness variation on the qinghai-tibetan plateau: historical and projected trends. Journal of Geophysical Research: Atmospheres, 126, e2021JD034841, https://doi.org/10.1029/2021JD034841, 2021.

Yang, Y., Wu, Q., Yun, H., Jin, H., and Zhang, Z.: Evaluation of the hydrological contributions of permafrost to the
540   thermokarst lakes on the Qinghai–Tibet Plateau using stable isotopes, Global and Planetary Change, 140, 1–8. https://doi.org/10.1016/j.gloplacha.2016.03.006, 2016.

Yao, T., Masson-Delmotte, V., Gao, J., Yu, W., Yang, X., Risi, C., Sturm, C., Werner, M., Zhao, H., He, Y., Ren, W., Tian, L., Shi, C., and Hou, S.: A review of climatic controls on $\delta^{18}O$ in precipitation over the Tibetan Plateau: Observations and simulations, Reviews of Geophysics, 51, 525–548, https://doi.org/10.1002/rog.20023, 2013.

545   Yang, Y., Wu, Q., Jin, H., Wang, Q., Huang, Y., Luo, D., Gao, S., and Jin, X..: Delineating the hydrological processes and hydraulic connectivities under permafrost degradation on Northeastern Qinghai-Tibet Plateau, China. Journal of Hydrology, 569, https://doi.org/10.1016/j.jhydrol.2018.11.068, 2018.

Zhao, L., Hu, G., Zou, D., Wu, X., and Liu, S.: Permafrost Changes and Its Effects on Hydrological Processes on Qinghai-Tibet Plateau. Bulletin of the Chinese Academy of Sciences, 34, 1233–1246, https://doi.org/10.16418/j.issn.1000-
550   3045.2019.11.006, 2019.

Zhou J., Liu, G., Meng, Y., Xia, C. C., and Chen, Y.: Using stable isotopes as tracer to investigate hydrological condition and estimate water residence time in a plain region, Chengdu, China. Scientific Reports, 11, https://doi.org/10.1038/s41598-021-82349-3, 2021.